Author for correspondence:
Ernest O. Asare
e-mail: ernest.asare@yale.edu

The influence of demographic and meteorological factors on temporal patterns of rotavirus infection in Dhaka, Bangladesh

Ernest O. Asare[1], Mohammad A. Al-Mamun[2], Monira Sarmin[3], A. S. G. Faruque[3], Tahmeed Ahmed[3] and Virginia E. Pitzer[1]

[1]Department of Epidemiology of Microbial Diseases, Yale School of Public Health, Yale University, New Haven, CT, USA
[2]Department of Pharmaceutical Systems and Policy, School of Pharmacy, West Virginia University, USA
[3]Nutrition and Clinical Services Division (NCSD), International Centre for Diarrheal Disease Research, Bangladesh (icddr,b), Dhaka, Bangladesh

EOA, 0000-0003-4078-8755

To quantify the potential impact of rotavirus vaccines and identify strategies to improve vaccine performance in Bangladesh, a better understanding of the drivers of pre-vaccination rotavirus patterns is required. We developed and fitted mathematical models to 23 years (1990–2012) of weekly rotavirus surveillance data from Dhaka with and without incorporating long-term and seasonal variation in the birth rate and meteorological factors. We performed external model validation using data between 2013 and 2019 from the regions of Dhaka and Matlab. The models showed good agreement with the observed age distribution of rotavirus cases and captured the observed shift in seasonal patterns of rotavirus hospitalizations from biannual to annual peaks. The declining long-term trend in the birth rate in Bangladesh was the key driver of the observed shift from biannual to annual winter rotavirus patterns. Meteorological indices were also important: a 1°C, 1% and 1 mm increase in diurnal temperature range, surface water presence and degree of wetness were associated with a 19%, 3.9% and 0.6% increase in the transmission rate, respectively. The model demonstrated reasonable predictions for both Dhaka and Matlab, and can be used to evaluate the impact of rotavirus vaccination in Bangladesh against changing patterns of disease incidence.

1. Introduction

Rotavirus remains an important diarrhoeal disease among children less than 5 years of age globally with significant morbidity and mortality in low- and middle-income countries (LMICs), particularly in sub-Saharan Africa and South Asia. Together, these two regions accounted for more than 85% of estimated global rotavirus deaths among children less than 5 years between 2000 and 2013 [1]. However, rotavirus vaccine impact has been found to be low to moderate in these regions [2]. In addition, the cost of treatment for rotavirus episodes imposes an economic burden on households in South Asia [3,4]. In order to quantify vaccine impact and identify strategies to improve both the performance and cost-effectiveness of rotavirus vaccines in these settings, a better understanding of the drivers of pre-vaccination rotavirus patterns is required.

In Bangladesh, rotavirus is the leading cause of severe diarrhoea, accounting for about two-thirds of acute gastroenteritis (AGE) hospitalizations and about 3% of all deaths among children less than 5 years old [5,6]. Rotavirus transmission occurs year-round with a predominant seasonal peak during the

dry season (November–February). Almost half of hospitaliz-ations occur among infants 6–11 months old [6,7]. Several studies reported an association of rotaviral diarrhoea with hypernatremia and convulsion in children [8]. The high mor-bidity but relatively low mortality rates in Bangladesh can be attributed in part to the widespread availability of oral rehy-dration salts for early treatment at home [9,10]; the future introduction of rotavirus vaccine is likely to further reduce the morbidity and mortality rate.

In Bangladesh, changes in the epidemiology of rotavirus such as increases in the proportion of diarrhoea attributable to rotavirus and genotype circulation have been reported [5,11,12]. In order to evaluate the impact of rotavirus vacci-nation against changing epidemiological patterns of disease burden, it is necessary to identify potential drivers of rota-virus incidence in the absence of vaccination. Some of these drivers of pre-vaccination rotavirus epidemiology could also interfere with vaccine performance and contribute to the differential rotavirus vaccine impact between and within LMICs and high-income settings [13–16].

A number of studies have attempted to assess the importance of demographic and environmental factors as potential drivers of the spatio-temporal pattern of rotavirus incidence [17–21]. For instance, Pitzer et al. [18] demonstrated that high birth rates in tropical countries may contribute to the observed lack of rota-virus seasonality in these settings. Nevertheless, meteorological variables are likely to influence rotavirus seasonal patterns. Temperature and rainfall have been found to be important fac-tors controlling both virus survival outside the host and dispersal and persistence in the environment [22,–24]. In South Asia, Jagai et al. [25] found an inverse relationship between both temperature and rainfall and the risk of rotavirus infections, while Hasan et al. [26] found a positive association between rotavirus and diurnal temperature variations.

While most modelling studies have assessed the impact of demographic and environmental factors independently, further studies are needed to assess their combined effects on rotavirus incidence. Here, we use mathematical models of rotavirus transmission dynamics to investigate the impor-tance of long-term and seasonal variations in the birth rate and meteorological indices, including diurnal temperature range (dtr), degree of wetness (dow) and surface water pres-ence (wpre), as potential drivers of temporal variations of rotavirus incidence in Dhaka, Bangladesh. We compared 23 years of observed weekly rotavirus cases with those pre-dicted by models with and without incorporating seasonal variation in the birth rate and meteorological indices. For the model to be used to evaluate future benefits of rotavirus vaccination in Bangladesh, it is important that the model can reproduce the observed pre-vaccination rotavirus patterns. Thus, the predictive potential of the models was assessed by performing external validation using weekly data between 2013 and 2019 from Dhaka and Matlab.

2. Methods and data

(a) Rotavirus data

Weekly records of confirmed rotavirus-positive cases for Dhaka were obtained from the International Centre for Diarrheal Disease Research, Bangladesh (icddr,b). The sur-veillance platform has been described previously [5,27,29]. Briefly, stool samples were collected from a systematic

sample of diarrhoeal patients presenting to iccdr,b hospital in Dhaka; every 25th patient (4%) was sampled between 1990 and 1995, while every 50th patient (2%) has been sampled since 1996. Stool samples were tested for rotavirus using ELISA. The rotavirus-positive cases were aggregated into 17 age groups (monthly intervals for infants less than 1-year-old, yearly intervals from 1 year to less than 5 years of age, and those aged 5 years or older). To examine the potential changes in rotavirus patterns over time, we divided the dataset into two parts: 1990–2001 (part 1) and 2003–2012 (part 2). The data for 2002 were used as a transition period to evaluate the best-fit models from the sub-data. In addition, the best-fit models were validated using weekly confirmed rotavirus-positive cases between 2013 and 2019 (part 3).

We also performed external model validation using weekly rotavirus surveillance data obtained from Matlab Hospital between 2013 and 2019. Matlab is a rural area situated 55 km southeast of Dhaka and forms part of the icddr,b's Diarrhoeal Disease Surveillance System (DDSS). Unlike Dhaka, stool samples are collected from all diarrhoeal patients coming from the DDSS area and attending the Matlab Hospital and tested for rotavirus using ELISA. Similar to Dhaka, the rotavirus-positive cases were aggregated into 17 age groups.

(b) Meteorological data and indices

Daily minimum and maximum 2 m air temperature data were obtained from the European Centre for Medium-Range Weather Forecasts (ECMWF) ERA-Interim reanalysis product [30], while daily rainfall data were obtained from Climate Hazards group Infrared Precipitation with Stations (CHIRPS) [31]. These are reanalysed data that combine model outputs with earth observational datasets. Previous studies have used hydrometeorological variables derived from these earth observations to predict rotavirus [32,33]. Both datasets were extracted over Dhaka and Matlab for the study period 1990–2019. We used these meteorological variables to derive three indices: diurnal temperature range (dtr), degree of wetness (dow) and surface water presence (wpre).

The daily dtr is given by

$$dtr = T_{max} - T_{min},$$ (2.1)

where T_{max} and T_{min} are the daily maximum and minimum temperatures, respectively. The daily dtr was normalized and then averaged to generate a weekly time series. We used dtr rather than temperature because it better captures the combined effects of cooler night-time temperatures and lower humidity, both of which favour virus survival [34]; fur-thermore, it demonstrated strong associations with rotavirus incidence in Dhaka in a previous analysis [26].

The weekly dow [35] is given by

$$dow = \frac{(\text{total rainfall per week}) \times (\text{number of rainy days per week})}{7}.$$ (2.2)

The dow was normalized before incorporating it into the model. We used the dow instead of actual rainfall to reduce sensitivity to isolated heavy storm events within a week.

The daily wpre is an output from a simple water balance model developed by Asare et al. [36,37] that requires only rainfall data and other estimated fluxes to predict fractional

coverage of surface water over a given area. The model equation is given by

$$\frac{\mathrm{d}w_{\mathrm{pond}}}{\mathrm{d}t} = \frac{2}{\rho h_{\mathrm{ref}}} \left(\frac{w_{\mathrm{ref}}}{w_{\mathrm{pond}}}\right)^{\rho/2} ((Q(w_{\mathrm{max}} - w_{\mathrm{pond}}) + P w_{\mathrm{pond}})(1-f) - w_{\mathrm{pond}}(E + fI_{\mathrm{max}})), \tag{2.3}$$

where w_{pond} is the daily fractional flood water coverage, ρ is the geometrical shape factor, w_{max} is the maximum flood water coverage, h_{ref} is the reference flood water depth, w_{ref} is the reference flood water coverage, Q (derived from the soil conservation service curve number method [38]) is the runoff, P is the rainfall, E is the evaporation, I_{max} is the maximum infiltration and $f = w_{\mathrm{pond}}/w_{\mathrm{max}}$. The values of the fixed model parameters are listed in the electronic supplementary material, table S1. The daily fractional flood water coverage was normalized and aggregated to generate a weekly time series. The *wpre* provides a proxy for flooding events.

Since *dow* and *wpre* are correlated and highest during the monsoon season, we evaluated them in separate models with *dtr*, which peaks in the winter season. To interpret the effect sizes associated with each meteorological variable, we multiplied by the standard deviation to convert back to the original scale.

(c) Demographic data

Data on long-term trends in the crude birth rate, crude death rate, average annual rate of population change and total population for Dhaka were obtained from the World Urbanization Prospects database [39]. We used linear interpolation to estimate values for the weekly birth and death rates per 1000 population, and estimated the net rate of immigration as the average annual rate of population change minus the difference between the crude annual birth and death rates. We verified that our model was able to reproduce the observed total size and age distribution of the Dhaka population over time.

To explore the potential impact of seasonality in the birth rate, we used data from a longitudinal study of about 2500 women across 14 villages in Matlab, Bangladesh that were followed for a period of 4 years [40]. As the birth seasonality in Dhaka is unknown, we assumed that it was either strongly seasonal as observed in Matlab or exhibited no seasonality. We fitted a sinusoidal function to the monthly birth rate data from Matlab to estimate the amplitude and timing (i.e. phase) of seasonality in the birth rate, then multiplied the resulting function by the birth rate of Dhaka to obtain the seasonal birth rate (equation 2.4) used in the models:

$$B_s(t) = B_{lt}(t) \times \left(1 + 0.42 \times \cos\left(\frac{2\pi t - 48}{52.18}\right)\right), \tag{2.4}$$

where B_s and B_{lt} are the seasonal and long-term trend in birth rates for Dhaka, respectively. We assumed that the amplitude and timing of birth seasonality remained consistent over time.

(d) Model description

We modified the mathematical model of rotavirus transmission developed by Pitzer *et al.* [17] (figure 1) to incorporate seasonal variation in the birth rate and meteorological indices. The model assumes that newborns enter the
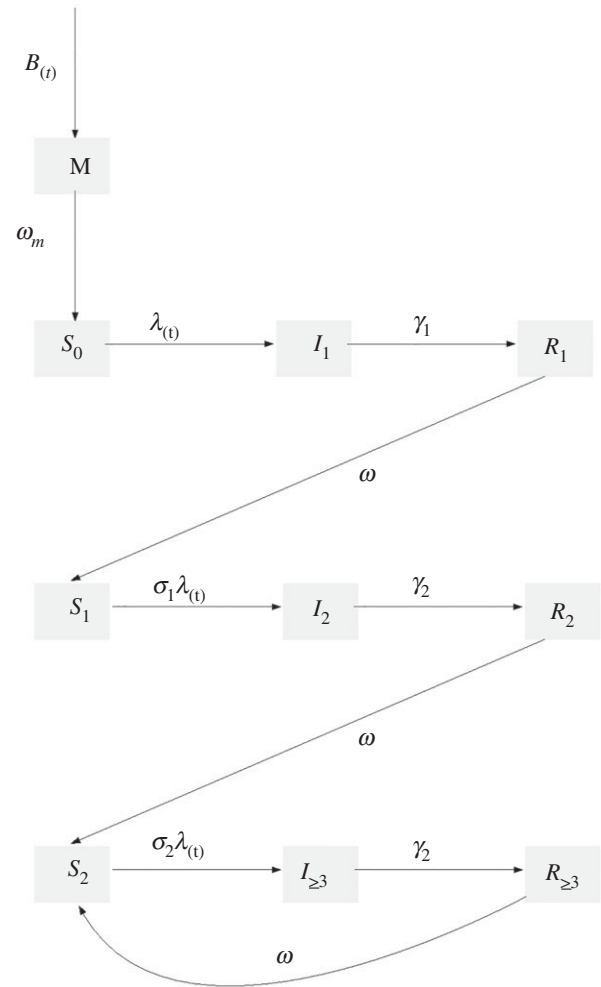
Figure 1. Schematic of the mathematic model for rotavirus transmission dynamics. Model parameters are described in electronic supplementary material, table S2.

maternal compartment M (which was divided into six subcompartments to account for non-exponential waning of maternal antibodies) at a rate equal to the birth rate B and are protected from rotavirus infection by maternal antibodies. This immunity wanes at a rate ω_m, after which infants become fully susceptible to primary infection (S_0). Primary infections occur at a rate λ, and infected individuals (I_1) remain infectious for an average period of $1/\gamma_1$, with a fraction (d_1) developing severe rotavirus diarrhoea. Recovered individuals enter the R_1 compartment and are assumed to have temporary immunity to reinfection that wanes at a rate ω. Following the waning of immunity, individuals become susceptible to secondary infection (S_1), which occur at a reduced rate $\sigma_1\lambda$. The secondary infected individuals (I_2) are less likely to develop severe diarrhoea (d_2), have lower infectiousness (by a factor ρ_2) and recover at a faster rate γ_2 into the R_2 compartment. Again, immunity wanes at the same rate ω, after which individuals move into the partially immune susceptible compartment (S_2); subsequent infections occur at a further reduced rate $\sigma_2\lambda$, but are assumed to be mostly asymptomatic or mildly symptomatic (proportion severe d_3 was estimated). The partially immune infected individuals ($I_{\geq 3}$) have infectiousness reduced by a factor $\rho_{\geq 3}$ and recover at a rate γ_2. The recovered individuals enter the $R_{\geq 3}$ compartment, where their immunity wanes at the same rate ω, after which individuals return to the S_2 compartment.

The force of infection (i.e. the rate of transmission from infected to susceptible individuals) at time t in weeks, $\lambda(t)$, is given by

$$\lambda(t) = \beta(t)(I_1(t) + \rho_2 I_2(t) + \rho_{\geq 3} I_{\geq 3}(t)), \quad (2.5)$$

where $\beta(t)$ is the seasonally varying transmission parameter. To determine the number of harmonic terms to include in the model, we performed wavelet analysis on the weekly rotavirus-positive time-series data for 1990–2019 and subsets of data divided into part 1 (1990–2001), part 2 (2003–2012) and part 3 (2013–2019; validation period).

For our default model (model 0), we assumed sinusoidal forcing with both annual and biannual harmonic terms (equation (2.6a)):

Model 0:

$$\beta(t) = \beta_0 \left(1 + b_1 \cos\left(\frac{2\pi t - \emptyset_1}{52.18}\right) + b_2 \cos\left(\frac{2\pi t - \emptyset_2}{26.09}\right) \right). \quad (2.6a)$$

We then extended this model to estimate the contribution of meteorological forcing in addition to the sinusoidal forcing, evaluating dtr and either dow (model A, equation (2.6b)) or $wpre$ (model B, equation (2.6c)) as best explaining the influence of rainfall:

Model A:

$$\beta(t) = \beta_0 \left(1 + b_1 \cos\left(\frac{2\pi t - \emptyset_1}{52.18}\right) + b_2 \cos\left(\frac{2\pi t - \emptyset_2}{26.09}\right) \right.$$
$$\left. + b_{dtr}(dtr) + b_{dow}(dow) \right), \quad (2.6b)$$

Model B:

$$\beta(t) = \beta_0 \left(1 + b_1 \cos\left(\frac{2\pi t - \emptyset_1}{52.18}\right) + b_2 \cos\left(\frac{2\pi t - \emptyset_2}{26.09}\right) \right.$$
$$\left. + b_{dtr}(dtr) + b_{wpr}(wpre) \right), \quad (2.6c)$$

where β_0 is the baseline transmission rate, b_1 is the amplitude of annual seasonal forcing, b_2 is the amplitude of biannual seasonal forcing, ϕ_1 is the annual seasonal offset, ϕ_2 is the biannual seasonal offset, b_{dtr} is the scaling parameter for dtr, b_{dow} is the scaling parameter for dow and b_{wpre} is the scaling parameter for $wpre$. The model input parameters are defined in the electronic supplementary material, table S2.

(e) Model-fitting approach

We fitted the models to the 23 years of weekly age-stratified rotavirus surveillance data from Dhaka Hospital using a maximum-likelihood framework; we estimated 8 to 10 parameters while fixing the remaining model parameters at values identified from the literature (see electronic supplementary material, table S2). We assumed that the confirmed cases of rotavirus in each week and age group followed a Poisson distribution with mean equal to the model-predicted number of severe rotavirus cases multiplied by an estimated reporting fraction (h). The 95% confidence intervals for parameters of interest (R_0, $1/\omega_m$, b_1, ϕ_1, b_2, ϕ_2, b_{dtr}, b_{dow} and b_{wpre}) were determined by profile likelihoods. We fitted the models with and without incorporating seasonal variation in the birth rate. The models were fitted to both the whole time series (complete: 1990–2012) and subsets of the data (part 1: 1990–2001 and part 2: 2003–2012) to estimate the model parameters. Finally, we performed external model validation by comparing model predictions to weekly rotavirus surveillance data between 2013

and 2019 from Dhaka and Matlab. We used demographic data for Matlab obtained from the World Urbanization Prospects database [39].

3. Results

The average annual incidence of rotavirus was more than 500 confirmed cases in Dhaka between 1990 and 2019. The highest number of confirmed rotavirus cases per week was 41 (figure 2a). Observed rotavirus cases showed a shift in seasonal patterns from predominantly biannual to annual peaks towards the end of the model-fitting period (1990–2012) (figure 2b). The annual epidemics persisted and increased in intensity during 2013–2019 (validation period) (figure 2b). Rotavirus cases occurred year-round, with the highest proportion of cases (46%) occurring during the winter months (November–February) and the peak occurring either in December or January. Minor peaks also usually occurred during the monsoon season (July–October), but occasionally during the pre-monsoon hot season (March–June), accounting for about 27% and 26% of the cases, respectively (figure 2c).

Comparing part 1 (1990–2001) and part 2 (2003–2012) (figure 2c), there was a slight increase in the proportion of cases occurring in the winter months (part 1: 41%; part 2: 45%) and a reduction in the proportion of cases occurring during the monsoon months (part 1: 32%; part 2: 26%). While there were more cases during the monsoon season than the pre-monsoon season in part 1, the proportion of cases in these two seasons were similar in part 2. Peak cases occurred in either December or January for part 1, but predominantly in January for part 2. For part 3 (validation period), more than half (55%) of rotavirus cases occurred during the winter months (figure 2c). There was a comparable proportion of cases occurring during the remaining periods (monsoon: 22%; pre-monsoon: 23%).

Figure 2d shows the temporal patterns of the demographic and meteorological drivers used for the model. The birth rate showed a consistent substantial decrease from 36 births per 1000 people in 1990 to 18 births per 1000 people in 2019. Diurnal temperature range peaked during winter, while both surface water presence and degree of wetness peaked during the monsoon periods (figure 2d).

All the models were able to reproduce the overall temporal patterns in rotavirus incidence, particularly the shift from biannual to annual seasonal peaks and the increasing trend in the peak season outbreaks of rotavirus towards the end of the study period (figure 3a). The models also performed well in estimating the proportion of rotavirus cases occurring in the winter and monsoon seasons (figures 2c and 3b). Table 1 summarizes the estimated parameter sets that provided the best fit to the complete data and the associated Bayesian information criterion (BIC) values. Based on the BIC, models incorporating both the seasonal birth rate, dtr and $wpre$ meteorological indices (model B_{sbr}) provided the best fit to the data (table 1). However, the models mostly underestimated the winter peaks in the early part of the study period, specifically 1994–1995 and 1997, and also failed to capture a notable monsoon outbreak in 2004 (figure 3a).

The proportion of rotavirus cases in the monthly less than 1-year-old age groups increased steadily until 8 months of age (figure 3c). Over half of the cases (51%) occurred in infants aged 5–11 months, while only 3% of cases occurred
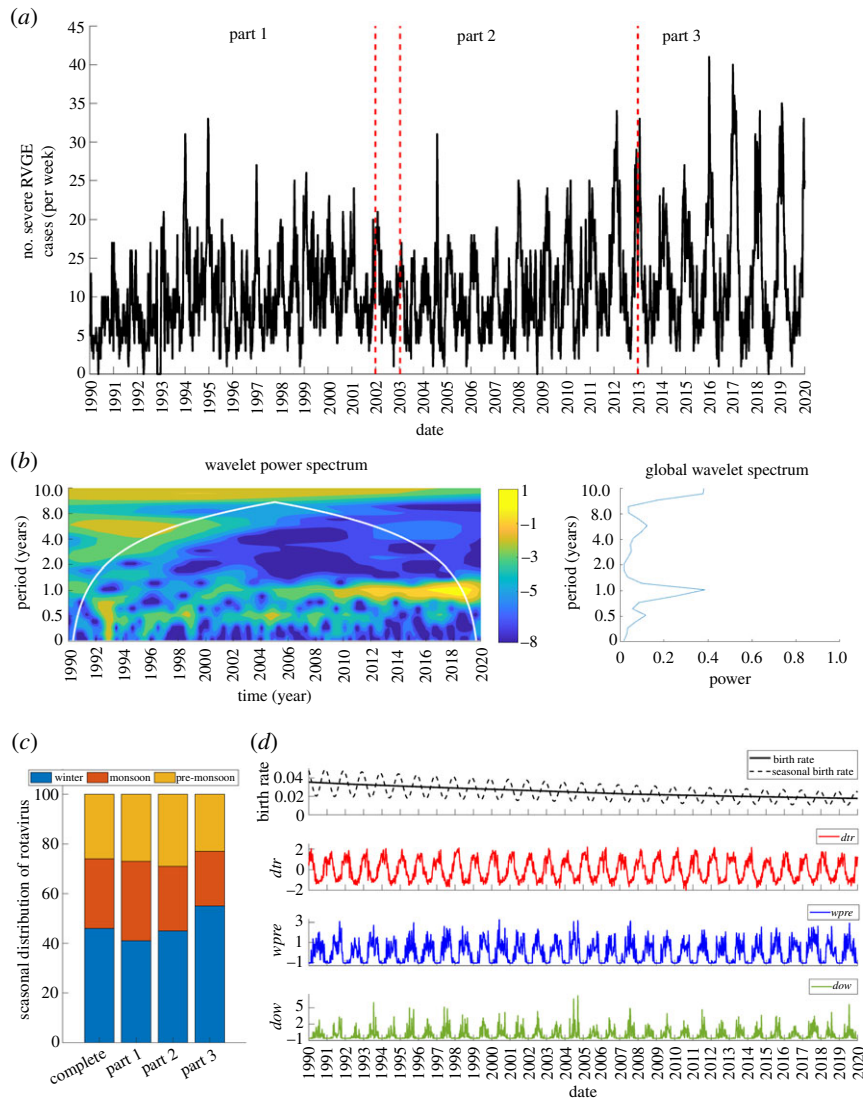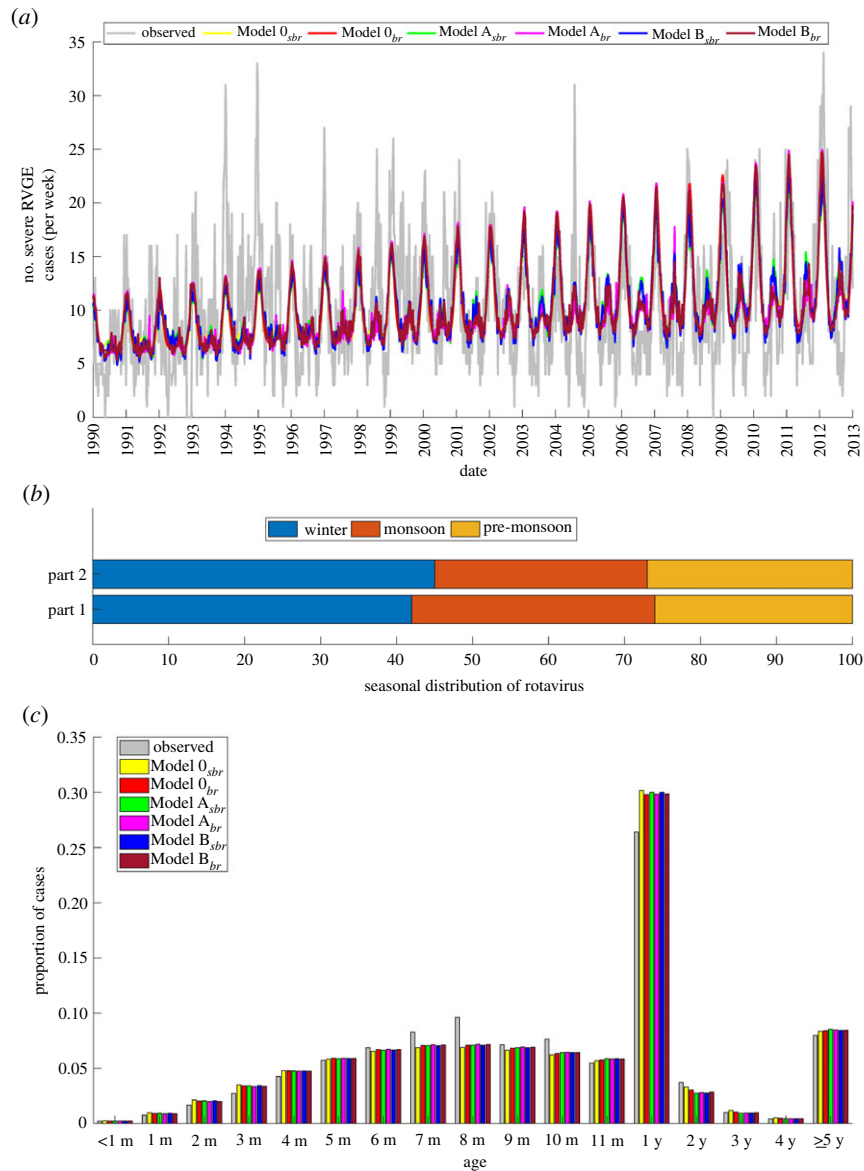
Figure 2. Time series of observed rotavirus cases and demographic and meteorological model inputs. (*a*) Weekly rotavirus cases in Dhaka between 1990 and 2019. The vertical lines indicate the three time periods (part 1: 1990–2001; part 2: 2003–2012 and part 3: 2013–2019). (*b*) The local and global wavelet spectrum of the weekly rotavirus cases. For the local wavelet power spectrum, blue corresponds to lowest intensity and yellow to the highest intensity. (*c*) Stacked bar plot showing the seasonal distribution of rotavirus cases for the complete and sub-divided datasets. (*d*) Weekly interpolated birth rate, corresponding seasonality in the birth rate, and normalized meteorological indices used in the model: diurnal temperature range (*dtr*), surface water presence (*wpre*) and degree of wetness (*dow*).

in infants less than 3 months of age. Only 5% of cases occurred in 2- to 4-year-olds, and 8% of cases were in persons aged greater than or equal to 5 years (figure 3*c*). Generally, the models were able to reproduce the observed age distribution patterns and accurately predicted both the trend and peak age of hospitalizations (8 months) for infants less than 1 year old (figure 3*c*). In addition, the models showed good agreement with the observed trend and proportion of cases in children aged 2–4 years and greater than or equal to 5 years (figure 3*c*). However, all models slightly overestimated the proportion of rotavirus cases in the 1-year-old age group and underestimated cases in the 7-, 8- and 10-month-old age groups.

Comparing part 1 and part 2, our models were able to estimate the timing of winter peaks and, in addition, the biannual and mostly annual outbreaks in part 1 and part 2 (figure 4*a,b*), respectively. The age distribution of rotavirus cases was similar in part 1 and part 2, which was consistent with the estimates from our models (electronic supplementary material, figure S1). Based on BIC, the best model for both part 1 and part 2 is the same model including a seasonal birth rate, *dtr* and *wpre* (electronic supplementary material,

table S3). Both best-fit models were able to predict weekly rotavirus patterns in 2002 (figure 4*c*). The best model for part 1 showed a remarkable agreement with the timing and intensity of the winter peak in 2002, but slightly overestimated the monsoon season rotavirus activity. On the other hand, the best-fit model for part 2 satisfactorily predicted monsoon rotavirus activity but underestimated the size of the winter peak.

The relative effect of the meteorological indices on the transmission rate, given by the scaling parameters (b_{dtr}, b_{dow}, b_{wpre}), was greatest for *dtr* (electronic supplementary material, table S4). A 1°C increase in *dtr* was associated with a 19% increase in the rotavirus transmission rate in the best-fit model; this effect was greater for part 2 (34%) compared to part 1 (2.3%). The *wpre* consistently contributed to a greater proportion of the transmission rate (3.9% for a 1% increase in *wpre*) compared to *dow* (0.6% for a 1 mm increase in *dow* for the model including seasonality in the birth rate). The effect estimates for *wpre* and *dow* were generally consistent between part 1 and part 2 (electronic supplementary material, table S4).

Figure 3. Comparison of model-simulated and observed rotavirus incidence in Dhaka for the complete dataset. (a) The weekly time series are plotted; the coloured lines correspond to the best-fit models, while the grey line corresponds to the observed data. (b) Comparison of the seasonal distribution of model-simulated rotavirus cases in part 1 and part 2. (c) Age distribution of rotavirus cases for the observed data (grey bars) and best-fit models (coloured bars).

The model validation showed that the best-fit model was able to accurately predict the observed peak timing, duration and intensity of rotavirus activity in winter for both Dhaka and Matlab (figure 5a,b). However, the best-fit model consistently overestimated rotavirus cases during the pre-monsoon and monsoon seasons. Based on mean absolute error, the best-fit model for part 2 has a slightly better predictive performance for both Dhaka and Matlab (Dhaka complete: 5.89, part 1: 5.33, part 2: 5.30; and Matlab complete: 3.68, part 1: 3.44, part 2: 3.40). The proportion of cases occurring during winter were comparable (Dhaka: 55%; Matlab: 54%), but the proportion of cases occurring in the monsoon season were higher in Matlab than Dhaka (figure 5c). The model underestimated and overestimated the proportion of cases occurring during the winter and monsoon seasons, respectively. The models were able to predict the observed trends in the age distribution but over- or underestimated the proportion of cases in some age groups (electronic supplementary material, figure S2).

The intensity of the biannual peak quantified by the wavelet power spectrum was greater than the annual in part 1 (biannual: 0.13; annual: 0.06), but the opposite was true for part 2 (biannual: 0.17; annual: 0.30) and part 3 (biannual: 0.03; annual: 0.85) (electronic supplementary material, figures S3a and S4a). Wavelet analysis of best-fit models with (electronic supplementary material, figure S3b) and without (electronic supplementary material, figure S3c) seasonality in the birth rate shows that both models were able to reproduce the observed shift from the predominantly biannual cycle in part 1 to a stronger annual signal in part 2. However, when we fitted the model assuming a fixed birth rate (using the average birth rate between 1990 and 2012) rather than the declining long-term trend in the birth rate, the model failed to reproduce the observed shift in rotavirus patterns (electronic supplementary material, figure S3d).

There is a substantial increase in the intensity of the annual signal in the validation period (2013–2019) compared to the fitting period for Dhaka (electronic supplementary material,

Table 1. The best-fit model parameters for the complete dataset (1990–2012). Values in parentheses indicate 95% confidence intervals. Here, sbr represents the models using seasonal birth rate, while br represents models assuming a non-seasonal birth rate. The best model (model B_{sbr}) is italicized. R_0: basic reproductive number, ω_m: duration of waning maternal immunity, d_3: proportion of subsequent infections that are severe, h: proportion of severe diarrhoea cases reported, b_1: amplitude of annual seasonal forcing, ϕ_1: annual seasonal offset, b_2: amplitude of biannual seasonal forcing, ϕ_2: biannual seasonal offset, b_{dtr}: scaling parameter for dtr, b_{dow}: scaling parameter for dow, b_{wpre}: scaling parameter for $wpre$ and BIC: Bayesian information criterion.

parameter	model 0		model A		model B	
	sbr	br	sbr	br	*sbr*	br
R_0	49 (48.6–49.5)	51.9 (51.1–52.8)	26.7 (26.5–27.0)	35.7 (35.2–36.4)	*26.2 (25.9–26.4)*	39.3 (38.8–40.1)
$1/\omega_m$ (weeks)	26.9 (26.5–27.2)	28.1 (27.6–28.5)	28.9 (28.5–29.2)	29.1 (28.6–29.5)	*28.7 (28.6–29.1)*	28.9 (28.4–29.3)
d_3	4.10×10^{-4}	3.90×10^{-4}	3.60×10^{-4}	3.70×10^{-4}	*3.60×10^{-4}*	3.70×10^{-4}
h	0.043	0.042	0.051	0.045	*0.051*	0.045
b_1	0.116 (0.115–0.118)	0.095 (0.088–0.101)	0.103 (0.098–0.126)	0.106 (0.092–0.116)	*0.114 (0.107–0.130)*	0.095 (0.086–0.106)
ϕ_1 (weeks)	10.8 (10.6–11.0)	12.6 (12.1–13.0)	4.761 (4.7–7.0)	11.8 (11.0–12.5)	*5.7 (5.4–8.6)*	11.9 (11.2–12.6)
b_2	0.022 (0.022–0.024)	0.023 (0.022–0.025)	0.046 (0.044–0.051)	0.036 (0.033–0.038)	*0.047 (0.045–0.050)*	0.032 (0.029–0.034)
ϕ_2 (weeks)	33.2 (33.0–33.5)	33.5 (33.2–33.8)	32.6 (32.2–32.8)	33.2 (32.8–33.5)	*32.5 (32.3–32.8)*	33.1 (32.75–33.4)
b_{dtr}			0.357 (0.354–0.364)	0.179 (0.172–0.187)	*0.367 (0.361–0.372)*	0.128 (0.122–0.136)
b_{dow}			0.148 (0.057–0.293)	0.843 (0.607–0.951)		
b_{wpre}					*0.244 (0.175–0.481)*	0.385 (0.266–0.495)
BIC	34 111	34 158	34 065	34 126	*34 036*	34 114

figure S4a). A similar predominant annual signal was observed for Matlab (electronic supplementary material, figure S4b). The best-fit model (model B_{sbr}) was able to predict the observed increase in annual seasonal epidemics of rotavirus (electronic supplementary material, figure S4c,d).

4. Discussion

Using mathematical models fitted to weekly rotavirus cases in Dhaka, we demonstrated for the first time that a consistent reduction in the birth rate over time in Bangladesh can help to explain the shift from biannual to annual seasonal patterns. Furthermore, seasonality in the birth rate and meteorological indices are important factors in capturing the amplitude and timing of seasonal peaks, particularly during the winter season. Overall the models demonstrated good performance in predicting both temporal patterns and the age distribution of rotavirus cases in Dhaka and Matlab.

The year-round circulation of rotavirus with major peaks during the winter season (November–February) in Dhaka is similar to what has been found in other parts of the country. Satter *et al.* [6] found that rotavirus contributes to more than 80% of acute AGE hospitalizations among children less than 5 years old between November and February across seven hospitals in Bangladesh. This also is consistent with what has been observed in other tropical regions [25,41].

In addition, we found a shift from biannual to nearly annual rotavirus incidence in Dhaka beginning around 2010, which our models were able to reproduce. Among the demographic and environmental variables considered, the declining long-term trend in the birth rate was identified as a key driver of this shift towards more annual seasonal epidemics. When we fitted the best model (model B_{sbr}) assuming a constant birth rate (using the average birth rate between 1990 and 2012), we could not reproduce the shift from biannual to annual epidemics (electronic

supplementary material, figures S3d and S5). This agrees with the study of Park *et al.* [20], who found a high birth rate as an important factor contributing to biannual peaks of rotavirus in Niger. The declining birth rate and an improvement in water treatment have also been hypothesized as potential drivers of a shift towards more seasonal rotavirus epidemics in Spain [42]. Similarly, Pitzer *et al.* [18] demonstrated that countries with lower birth rates tended to experience stronger seasonal rotavirus patterns compared to countries with higher birth rates. There was no significant difference in the meteorological indices between part 1 and part 2 (electronic supplementary material, figure S6), although we found that *dtr* may be contributing more to seasonality in rotavirus transmission during the latter part of the study period. For instance, while there was a more than 14-fold difference in the relative effect of *dtr* on the transmission rate between part 1 and part 2, comparable effects were found for *wpre* and *dow* for the two parts. Given that *dtr* is a useful indicator of climate change, its potential effects on rotavirus incidence under climate change, combined with changes in demographic characteristics, require further detailed investigation. Nevertheless, it is possible that factors such as improvements in sanitation and nutrition [11,43] and changes in rotavirus genotype circulation [44] may play a role in the altered transmission patterns. Future studies should explore whether these factors also contribute to the observed changes in rotavirus patterns.

Comparing models with and without seasonality in the birth rate revealed that the inclusion of seasonal births substantially improved the fit of the models based on BIC scores (table 1; electronic supplementary material, table S3). Although we only had data on birth seasonality in Matlab from the late 1970s, it is possible that seasonality in the birth rate in Bangladesh is substantial. The timing of the birth peak in November (electronic supplementary material, figure S7) may increase the availability of susceptible infants in the winter season, after maternal antibodies have waned, thereby facilitating the winter outbreaks. Since a high proportion of
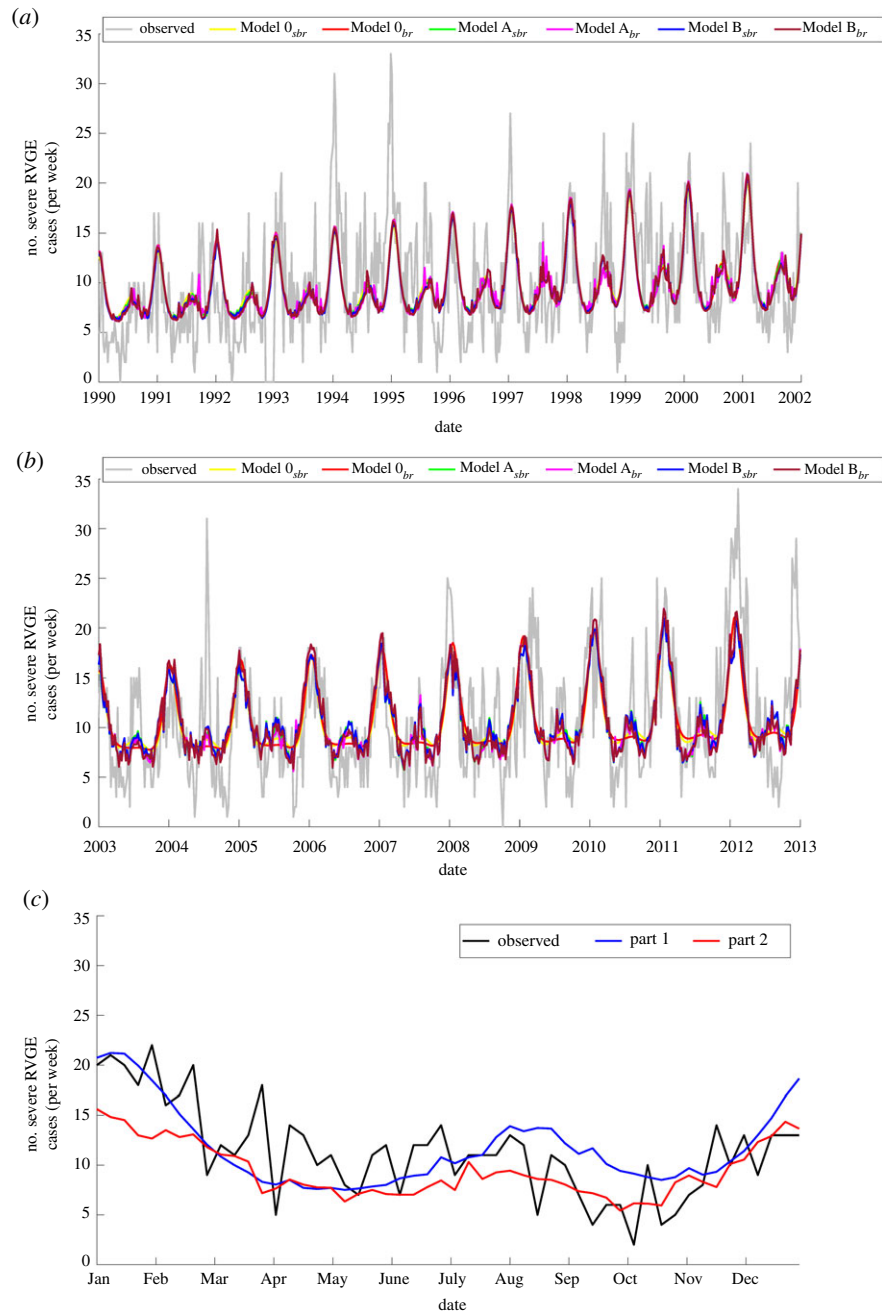
Figure 4. Comparison of models fitted to observed weekly rotavirus cases for during 1990–2001 and 2003–2012 and out-of-sample model validation for 2002. The observed (grey) and model-fitted (coloured lines) number of weekly rotavirus cases was plotted for (*a*) part 1 (1990–2001) and (*b*) part 2 (2003–2012) time series. (*c*) Observed and predicted weekly rotavirus cases in 2002 for the best-fit models (for part 1 and part 2). The comparison of the observed and model-fitted age distributions for part 1 and part 2 are in the electronic supplementary material, figure S1.

susceptible infants are infected during the winter period, there will be fewer susceptible infants remaining after the winter peak season, particularly during the latter part of the study period (2003–2012) and during the model validation period (2013–2019) when birth rates were lower, leading to decreasing monsoon peaks. Other studies have also demonstrated the importance of birth seasonality in predicting the timing and amplitude of measles epidemics [45,46].

The meteorological indices may also play an important role in predicting the timing of rotavirus epidemics, which predominately occur in January in Dhaka. Thus, meteorological indices derived from earth observations can be incorporated into dynamical models to improve predictions of rotavirus infections. Rotavirus survival is enhanced during cold dry periods, which is supported by the large coefficient of *dtr* estimated for part 2 and the consistency in the peak in *dtr* and

rotavirus incidence (electronic supplementary material, figure S6). Other studies have shown that rotavirus peaks in the dry cold period in the tropics and exhibits inverse associations with rainfall, temperature and relative humidity [25,41]. However, variation in the susceptible population likely influences the disease seasonality. This is consistent with findings by Martinez *et al*. [19] who, using the same flood forcing, found differences in population density as a key driver of the observed differences in rotavirus seasonality between the main Dhaka city and peripheral towns surrounding it.

Contrary to the shift in temporal patterns of rotavirus from the 1990s to the 2000s, there was no significant change in the age distribution. The stable age distribution provides the basis for future examination of how vaccination could shift the age distribution of rotavirus cases. There is an agreement between the observed (60%) and predicted (56–58%)
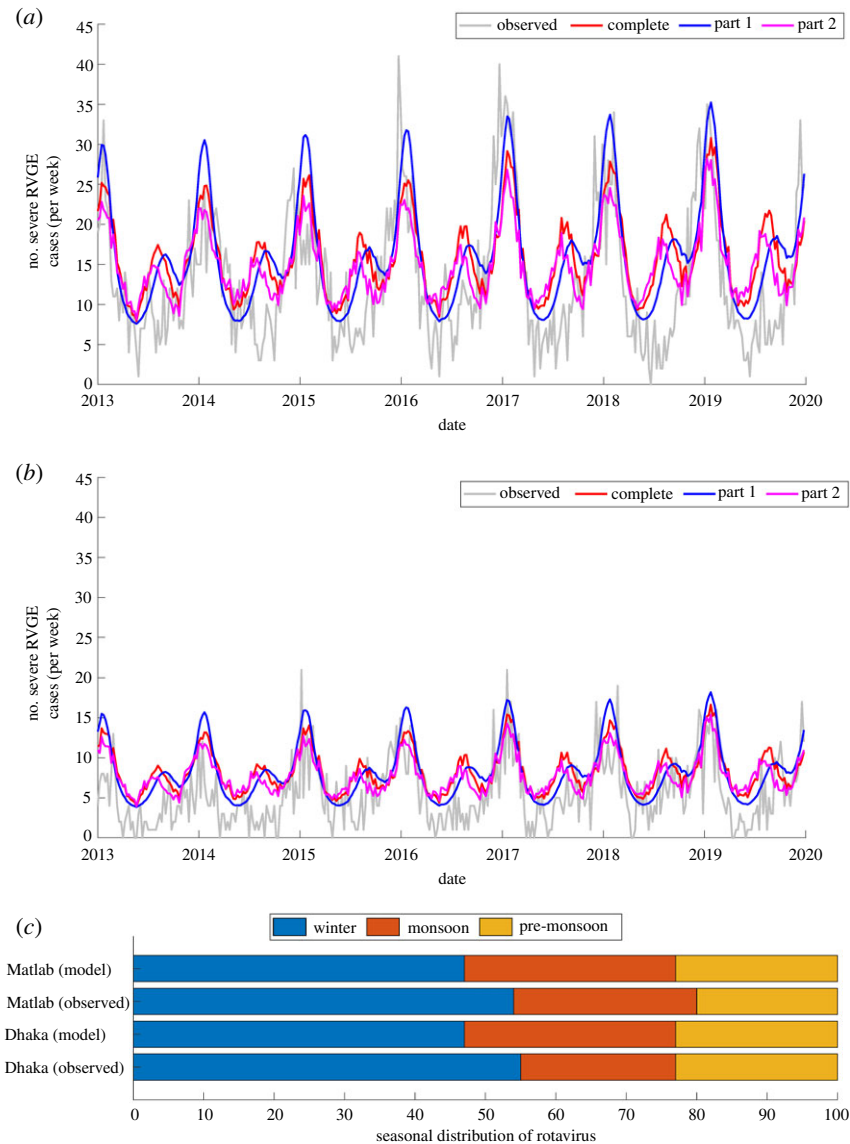
Figure 5. Comparison of model-predicted and observed weekly rotavirus time-series for external model validation. (*a*) Out-of-sample model validation using data from Dhaka. (*b*) External model validation using data from Matlab. (*c*) Comparison of the best-fit model-simulated and observed seasonal distribution in rotavirus cases for both Dhaka and Matlab. In both instances, the best-fit model (model B_{sbr}) was used. (Online version in colour.)

proportion of cases among children aged less than 12 months, which is similar to that reported for other LMICs (56–69%) [47–50], but higher than the range reported in high-income countries (41–55%) [51,52] prior to vaccine introduction. The small proportion of cases in infants less than 3 months (approx. 3%) agrees with the 3% observed globally [50] and suggests that the vast majority of rotavirus cases could be prevented using an infant vaccine schedule. Approximately 8% of cases occurred in the greater than or equal to 5 age group (figure 3*c*; electronic supplementary material, figure S1), which is similar to what has been reported in other parts of Bangladesh as well as in other countries [53–55]. This clearly shows that rotavirus continues to contribute to the burden of diarrhoea in older children and adults, and thus there is a need for a better understanding of how all age groups contribute to the burden and transmission of rotavirus both pre- and post-vaccination.

The models provide satisfactory predictions of the trend towards increasingly winter seasonal peaks of rotavirus observed in both Dhaka and Matlab during the validation period (2013–2019). The pronounced shift towards annual epidemics compared to biannual epidemics observed

during the model-fitting period is likely due to further declines in the birth rate. The crude birth rate decreased by about 2.5% between 2012 and 2019. Overall, the ability of the model to reliably predict rotavirus dynamics in Dhaka (urban) and Matlab (rural) provides confidence that the model can be used to investigate the impact of changes in birth rates on rotavirus patterns in other settings.

To identify effective vaccination strategies and evaluate vaccine impact, a better understanding of pre-vaccination rotavirus incidence is required. However, this is difficult if the patterns of rotavirus incidence are changing over time, as in the case of Dhaka. Our model provides a way of simulating rotavirus incidence in the absence of vaccination that accounts for the changing patterns in rotavirus epidemiology, thus providing a baseline against which to evaluate future vaccine impact. In addition, the model can also be used to evaluate the potential impact of different vaccination strategies to identify the optimal strategy for Bangladesh.

Our results add to the evidence of the importance of the changes in birth rates in controlling the temporal shift from biannual to annual rotavirus activity. The satisfactory agreement between the model and observed data from both

Dhaka and Matlab achieved during model validation demonstrates the potential of the models to predict the future dynamics of rotavirus in the absence of vaccination. The lack of substantial decline in rotavirus cases in Dhaka and Matlab despite a consistent long-term decline in birth rate justifies the need for introduction of rotavirus vaccine in Bangladesh. The models we have developed and validated demonstrate the potential for use in evaluation of the impact of rotavirus vaccination in Bangladesh against the changing patterns of rotavirus incidence.

Ethics. This is a secondary data analysis. Institutional Review Board (composed of Research Review Committee and Ethics Review Committee) has approved the study. Protocol no. is 19049. For primary activity, informed consent to participate from each of the participants was taken.

Data accessibility. The Institutional Review Board of icddr,b has the right to share data upon request. Data requests may be sent to Ms Armana Ahmed (aahmed@icddrb.org), head, Research Administration. Electronic supplementary material is available online [56].

Authors' contributions. E.O.A.: conceptualization, data curation, formal analysis, investigation, methodology, software, validation, visualization, writing—original draft and writing—review and editing; M.A.A.: data curation, formal analysis, investigation, visualization and writing—review and editing; M.S.: data curation and writing—

review and editing; A.S.G.F.: data curation and writing—review and editing; T.A.: data curation and writing—review and editing; V.E.P.: conceptualization, data curation, funding acquisition, investigation, supervision and writing—review and editing.

All authors gave final approval for publication and agreed to be held accountable for the work performed therein.

References

1. Tate JE, Burton AH, Boschi-Pinto C, Parashar UD. 2016 Global, regional, and national estimates of rotavirus mortality in children <5 years of age, 2000–2013. Clin. Infect. Dis. 62, S96–S105. (doi:10.1093/cid/civ1013)

2. Burnett E, Parashar U, Tate J. 2018 Rotavirus vaccines: effectiveness, safety, and future directions. Pediatr. Drugs 20, 223–233. (doi:10.1007/s40272-018-0283-3)

3. Kawai K, OBrien MA, Goveia MG, Mast TC, El Khoury AC. 2012 Burden of rotavirus gastroenteritis and distribution of rotavirus strains in Asia: systematic review. Vaccine 30, 1244–1254. (doi:10.1016/j.vaccine.2011.12.092)

4. Rheingans R, Kukla M, Faruque ASG, Sur D, Zaidi AKM, Nasrin D, Farag TH, Levine MM, Kotloff KL. 2012 Determinants of household costs associated with childhood diarrhea in South Asian settings. Clin. Infect. Dis. 55, S327–S335. (doi:10.1093/cid/cis764)

5. Tanaka G, Faruque AS, Luby SP, Malek MA, Glass RI, Parashar UD. 2007 Deaths from rotavirus disease in Bangladeshi children: estimates from hospital-based surveillance. Pediatr. Infect. Dis. J. 26, 1014–2018. (doi:10.1097/INF.0b013e318125721c)

6. Satter SM, Gastanaduy PA, Islam K, Rahman M, Rahman M, Luby SP, Heffelfinger JD, Parashar UD, Gurley ES. 2017 Hospital-based surveillance for rotavirus gastroenteritis among young children in Bangladesh: defining the potential impact of a rotavirus vaccine. Pediatr. Infect. Dis. J. 36, 168–172. (doi:10.1097/INF.0000000000001381)

7. Kilgore PE, Unicomb LE, Gentsch JR, Albert MJ, McElroy CA, Glass RI. 1996 Neonatal rotavirus infection in Bangladesh: strain characterization and risk factors for nosocomial infection. Pediatr. Infect. Dis. J. 15, 672–677. (doi:10.1097/00006454-199608000-00007)

8. Kaiser P, Borte M, Zimmer KP, Huppertz HI. 2012 Complications in hospitalized children with acute gastroenteritis caused by rotavirus: a retrospective analysis. Eur. J. Pediatr. 171, 337–345. (doi:10.1007/s00431-011-1536-0)

9. Larson CP, Saha UR, Nazrul H. 2009 Impact monitoring of the national scale up of zinc treatment for childhood diarrhea in Bangladesh: repeat ecologic surveys. PLoS Med. 6, e1000175. (doi:10.1371/journal.pmed.1000175)

10. Das SK et al. 2013 Health care-seeking behavior for childhood diarrhea in Mirzapur, rural Bangladesh. Am. J. Trop. Med. Hyg. 89, 62–68. (doi:10.4269/ajtmh.13-0107)

11. Sarker MHR et al. 2014 Changing characteristics of rotavirus diarrhea in children younger than five years in urban Bangladesh. PLoS ONE 9, e105978. (doi:10.1371/journal.pone.0105978)

12. Haque W et al. 2018 Distribution of rotavirus genotypes in Dhaka, Bangladesh, 2012–2016: re-emergence of G3P [8] after over a decade of interval. Vaccine 36, 6393–6400. (doi:10.1016/j.vaccine.2018.08.081)

13. Asare EO, Al-Mamun MA, Armah GE, Lopman BA, Parashar UD, Binka F, Pitzer VE. 2020 Modeling of rotavirus transmission dynamics and impact of vaccination in Ghana. Vaccine 38, 4820–4828. (doi:10.1016/j.vaccine.2020.05.057)

14. Velasquez DE, Parashar U, Jiang B. 2018 Decreased performance of live attenuated, oral rotavirus vaccines in low-income settings: causes and contributing factors. Expert Rev. Vaccines 17, 145–161. (doi:10.1080/14760584.2018.1418665)

15. Gruber JF, Becker-Dreps S, Hudgens MG, Brookhart MA, Thomas JC, Funk MJ. 2018 Timing of rotavirus vaccine doses and severe rotavirus gastroenteritis among vaccinated infants in low-and middle-income countries. Epidemiology 29, 867–875. (doi:10.1097/EDE.0000000000000909)

16. Steele A, Victor JC, Carey ME, Tate JE, Atherly DE, Pecenka C, Diaz Z, Parashar UD, Kirkwood CD. 2019 Experiences with rotavirus vaccines: can we improve rotavirus vaccine impact in developing countries? Hum. Vaccin. Immunother. 15, 1215–1227. (doi:10.1080/21645515.2018.1553593)

17. Pitzer VE et al. 2009 Demographic variability, vaccination, and the spatiotemporal dynamics of rotavirus epidemics. Science 325, 290–294. (doi:10.1126/science.1172330)

18. Pitzer VE, Viboud C, Lopman BA, Patel MM, Parashar UD, Grenfell BT. 2011 Influence of birth rates and transmission rates on the global seasonality of rotavirus incidence. J. R. Soc. Interface 8, 1584–1593. (doi:10.1098/rsif.2011.0062)

19. Martinez PP, King AA, Yunus M, Faruque A, Pascual M. 2016 Differential and enhanced response to climate forcing in diarrheal disease due to rotavirus across a megacity of the developing world. Proc. Natl Acad. Sci. USA 113, 4092–4097. (doi:10.1073/pnas.1518977113)

20. Park J, Goldstein J, Haran M, Ferrari M. 2017 An ensemble approach to predicting the impact of vaccination on rotavirus disease in Niger. Vaccine 35, 5835–5841. (doi:10.1016/j.vaccine.2017.09.020)

21. Kraay AN, Brouwer AF, Lin N, Collender PA, Remais JV, Eisenberg JN. 2018 Modeling environmentally mediated rotavirus transmission: the role of temperature and hydrologic factors. Proc. Natl Acad. Sci. USA 115, E2782–E2790. (doi:10.1073/pnas.1719579115)

22. Hashizume M, Armstrong B, Wagatsuma Y, Faruque A, Hayashi T, Sack DA. 2008 Rotavirus infections and

climate variability in Dhaka, Bangladesh: a time-series analysis. *Epidemiol. Infect.* **136**, 1281–1289. (doi:10.1017/S0950268807009776)

23. Sumi A, Rajendran K, Ramamurthy T, Krishnan T, Nair GB, Harigane K, Kobayashi N. 2013 Effect of temperature, relative humidity and rainfall on rotavirus infections in Kolkata, India. *Epidemiol. Infect.* **141**, 1652–1661. (doi:10.1017/S0950268812002208)

24. Levy K, Woster AP, Goldstein RS, Carlton EJ. 2016 Untangling the impacts of climate change on waterborne diseases: a systematic review of relationships between diarrheal diseases and temperature, rainfall, flooding, and drought. *Environ. Sci. Technol.* **50**, 4905–4922. (doi:10.1021/acs.est.5b06186)

25. Jagai JS, Sarkar R, Castronovo D, Kattula D, Mcentee J, Ward H, Kang G, Naumova EN. 2012 Seasonality of rotavirus in South Asia: a meta-analysis approach assessing associations with temperature, precipitation, and vegetation index. *PLoS ONE* **7**, e38168. (doi:10.1371/journal.pone.0038168)

26. Hasan MA, Mouw C, Jutla A, Akanda AS. 2018 Quantification of rotavirus diarrheal risk due to hydroclimatic extremes over South Asia: prospects of satellite-based observations in detecting outbreaks. *Geohealth* **2**, 70–86. (doi:10.1002/2017GH000101)

27. Stoll BJ, Glass RI, Huq MI, Khan M, Holt JE, Banu H. 1982 Surveillancepatients attending a diarrhoeal disease hospital in Bangladesh. *Br. Med. J. (Clin Res Ed)* **285**, 1185–1188. (doi:10.1136/bmj.285.6349.1185)

28. Unicomb LE, Kilgore P, Faruque ASG, Hamadani J, Fuchs G, Albert M, Glass R. 1997 Anticipating rotavirus vaccines: hospital-based surveillance for rotavirus diarrhea and estimates of disease burden in Bangladesh. *Pediatr. Infect. Dis. J.* **16**, 947–951. (doi:10.1097/00006454-199710000-00008)

29. Schwartz BS et al. 2006 Diarrheal epidemics in Dhaka, Bangladesh, during three consecutive floods: 1988, 1998, and 2004. *Am. J. Trop. Med. Hyg.* **74**, 1067–1073. (doi:10.4269/ajtmh.2006.74.1067)

30. Dee DP et al. 2011 The ERA-interim reanalysis: configuration and performance of the data assimilation system. *Q. J. R. Meteorol. Soc.* **137**, 553–597. (doi:10.1002/qj.828)

31. Funk C et al. 2015 The climate hazards infrared precipitation with stations-a new environmental record for monitoring extremes. *Sci. Data* **2**, 150066. (doi:10.1038/sdata.2015.66)

32. Colston JM et al. 2019 Use of earth observation-derived hydrometeorological variables to model and predict rotavirus infection (MAL-ED): a multisite cohort study. *Lancet Planet Health* **3**, e248–e258. (doi:10.1016/S2542-5196(19)30084-1)

33. Colston JM et al. 2022 Associations between eight earth observation-derived climate variables and enteropathogen infection: an independent participant data meta-analysis of surveillance studies with broad spectrum nucleic acid diagnostics. *Geohealth* **6**, e2021GH000452. (doi:10.1029/2021GH000452)

34. Ansari SA, Springthorpe VS, Sattar SA. 1991 Survival and vehicular spread of human rotaviruses: possible relation to seasonality of outbreaks. *Rev. Infect. Dis.* **13**, 448–461. (doi:10.1093/clinids/13.3.448)

35. Spencer CL. 1911 The sugar industry of Mauritius: a study in correlation including a scheme of insurance of the cane crop against damage caused by cyclones. *Nature* **87**, 344. (doi:10.1038/087344a0)

36. Asare EO, Tompkins AM, Amekudzi LK, Ermert V. 2016 A breeding site model for regional, dynamical malaria simulations evaluated using in situ temporary ponds observations. *Geospat. Health* **11**, 390. (doi:10.4081/gh.2016.390)

37. Asare EO, Tompkins AM, Bomblies A. 2016 A regional model for malaria vector developmental habitats evaluated using explicit, pond-resolving surface hydrology simulations. *PLoS ONE* **11**, e0150626. (doi:10.1371/journal.pone.0150626)

38. United States. Soil Conservation Service. 1972 SCS National Engineering Handbook, §4: Hydrology. See https://books.google.com/books?id=Tx5gzgAACAAJ.

39. United Nations Department of Economic and Social Affairs, Population Division. 2019 World population prospects 2019, online edition. Rev. 1. See https://population.un.org/wpp/Download/Standard/Population/.

40. Becker S, Chowdhury A, Leridon H. 1986 Seasonal patterns of reproduction in Matlab, Bangladesh. *Popul. Stud.* **40**, 457–472. (doi:10.1080/0032472031000142356)

41. Levy K, Hubbard AE, Eisenberg JN. 2009 Seasonality of rotavirus disease in the tropics: a systematic review and meta-analysis. *Int. J. Epidemiol.* **38**, 1487–1496. (doi:10.1093/ije/dyn260)

42. Cilla G, Pérez-Trallero E, López-Lopategui MC, Gilsetas A, Gomáriz M. 2000 Incidence, seasonality and serotypes of rotavirus in Gipuzkoa (Basque Country), Spain: a 14-year study. *2000 Epidemiol. Infect* **125**, 677–683. (doi:10.1017/s0950268800004842)

43. Dewan N, Faruque A, Fuchs G. 1998 Nutritional status and diarrhoeal pathogen in hospitalized children in Bangladesh. *Acta Paediatr.* **87**, 627–730. (doi:10.1080/080352598750014012)

44. Rahman M et al. 2007 Prevalence of G2P [4] and G12P [6] rotavirus, Bangladesh. *Emerg. Infect. Dis.* **13**, 18–24. (doi:10.3201/eid1301.060910)

45. Dorélien AM, Ballesteros S, Grenfell BT. 2013 Impact of birth seasonality on dynamics of acute immunizing infections in Sub-Saharan Africa. *PLoS ONE* **8**, e75806. (doi:10.1371/journal.pone.0075806)

46. Martinez-Bakker M, Bakker KM, King AA, Rohani P. 2014 Human birth seasonality: latitudinal gradient and interplay with childhood disease dynamics. *Proc. R. Soc. B* **281**, 20132438. (doi:10.1098/rspb.2013.2438)

47. Van Man N et al. 2001 The epidemiology and disease burden of rotavirus in Vietnam: sentinel surveillance at 6 hospitals. *Int. J. Infect. Dis.* **183**, 1707–1712. (doi:10.1086/320733)

48. Schael IP, González R, Salinas B. 2009 Severity and age of rotavirus diarrhea, but not socioeconomic conditions, are associated with rotavirus seasonality in Venezuela. *J. Med. Virol.* **81**, 562–567. (doi:10.1002/jmv.21420)

49. Tagbo B et al. 2018 Rotavirus diarrhoea hospitalizations among children under 5 years of age in Nigeria, 2011–2016. *Vaccine* **36**, 7759–7764. (doi:10.1016/j.vaccine.2018.03.084)

50. Hasso-Agopsowicz M et al. 2019 Global review of the age distribution of rotavirus disease in children aged <5 years before the introduction of rotavirus vaccination. *Clin. Infect. Dis.* **69**, 1071–1078. (doi:10.1093/cid/ciz060)

51. Zeller M et al. 2010 Rotavirus incidence and genotype distribution before and after national rotavirus vaccine introduction in Belgium. *Vaccine* **28**, 7507–7513. (doi:10.1016/j.vaccine.2010.09.004)

52. Jayasinghe S, Macartney K. 2013 Estimating rotavirus gastroenteritis hospitalisations by using hospital episode statistics before and after the introduction of rotavirus vaccine in Australia. *Vaccine* **31**, 967–972. (doi:10.1016/j.vaccine.2012.11.099)

53. Sanekata T, Ahmed MU, Kader A, Taniguchi K, Kobayashi N. 2003 Human group B rotavirus infections cause severe diarrhea in children and adults in Bangladesh. *J. Clin. Microbiol.* **41**, 2187–2190. (doi:10.1128/JCM.41.5.2187-2190.2003)

54. Carraro E, Perosa AHS, Siqueira I, Pasternak J, Martino MDV. 2008 Rotavirus infection in children and adult patients attending in a tertiary hospital of São Paulo, Brazil. *Braz. J. Infect. Dis.* **12**, 44–46. (doi:10.1590/s1413-86702008000100010)

55. Pietruchinski E et al. 2006 Rotavirus diarrhea in children and adults in a southern city of Brazil in 2003: distribution of G/P types and finding of a rare G12 strain. *J. Med. Virol.* **78**, 1241–1249. (doi:10.1002/jmv.20686)

56. Asare EO, Al-Mamun MA, Sarmin M, Faruque ASG, Ahmed T, Pitzer VE. 2022 The influence of demographic and meteorological factors on temporal patterns of rotavirus infection in Dhaka, Bangladesh. Figshare. (doi:10.6084/m9.figshare.c.6009332)